

Unintegrated partons to describe the P_T distributions of electroweak bosons at hadron colliders

G. WATT

Institute for Particle Physics Phenomenology, University of Durham, DH1 3LE, UK

Abstract

We describe the use of unintegrated parton distributions in hadron-hadron collisions, using the (z, k_t) -factorisation prescription where the transverse momentum of the incoming parton is generated in the last evolution step. We apply this formalism to calculate the transverse momentum (P_T) distributions of produced W and Z bosons, where the leading order contribution comes from quark-antiquark annihilation, and compare the predictions to Tevatron Run 1 data. We also predict the P_T distribution of the Standard Model Higgs boson at the LHC, where the dominant production mechanism is by gluon-gluon fusion.

1 Introduction

At present, it is not straightforward to describe the transverse momentum (P_T) distributions of electroweak bosons produced in hadron-hadron collisions. In the usual collinear approximation, the transverse momentum of the incoming partons is neglected and so, for the Born level subprocesses $q_1 q_2 \rightarrow V$ (where $V = \gamma^*, W, Z$) or $g_1 g_2 \rightarrow H$, the transverse momentum of the final electroweak boson is zero. Therefore, initial state QCD radiation is necessary to generate the P_T distributions. Both the leading order (LO) and next-to-leading order (NLO) differential cross sections diverge for $P_T \ll M_{V,H}$, with terms proportional to $\ln(M_{V,H}/P_T)$ appearing due to soft and collinear gluon emission, requiring resummation to achieve a finite P_T distribution. Current calculations combine fixed-order perturbation theory at high P_T with gluon resummation formalisms at low P_T , with some matching criterion to decide when to switch between the two. In addition, a parameterisation is needed to account for non-perturbative effects at the lowest P_T values. Resummation can be performed either in the

transverse momentum space (see [1], and references therein) or in the Fourier conjugate impact parameter space (see [2], and references therein).

An alternate description is provided in terms of *unintegrated* parton distribution functions (UPDFs), where each incoming parton carries its own transverse momentum, so that the subprocesses $q_1 q_2 \rightarrow V$ and $g_1 g_2 \rightarrow H$ already generate the LO P_T distributions. It has been shown [3] that UPDFs obtained from an approximate solution of the CCFM equation [4] embody the conventional soft gluon resummation formulae.

UPDFs may be obtained [5] from the conventional integrated PDFs determined from global analysis, assuming that the transverse momentum of the parton is generated entirely in the last evolution step. This formalism was extended in [6] where it was shown that it is necessary to consider *doubly*-unintegrated parton distribution functions (DUPDFs) to preserve the exact kinematics. It was demonstrated that the main features of conventional higher order calculations can be accounted for within a much simpler theoretical framework, named (z, k_t) -factorisation. The DUPDFs include a Sudakov form factor which resums the virtual terms in the DGLAP equation, and impose angular-ordering constraints which regulate the singularities arising from soft gluon emission. Therefore, there is a hope that (z, k_t) -factorisation may be used to achieve a unified description of the P_T distribution over the entire P_T range. In some sense, this idea is an extension of the original DDT formula [7]; however, in comparison with [7] we go beyond the double leading logarithmic approximation (DLLA), and account for the precise kinematics of the two incoming partons, as well as the angular ordering of emitted gluons.

In this paper we apply (z, k_t) -factorisation at LO to calculate the P_T distributions of W and Z bosons produced at the Tevatron Run 1, and compare the predictions to data taken by the CDF and DØ Collaborations. We also calculate the P_T distribution of Standard Model (SM) Higgs bosons produced at the LHC.

2 (z, k_t) -factorisation at hadron-hadron colliders

We now extend the formalism of [6], which concerned deep-inelastic scattering (DIS), to hadron-hadron collisions. The basic idea is illustrated in Fig. 1(a), which shows only one of the possible configurations. All permutations of quarks and gluons must be included. The arrows show the direction of the labelled momenta. The blobs represent the conventional integrated PDFs. The transverse momenta of the two incoming partons to the subprocess, represented by the rectangles labelled $\hat{\sigma}^{q_1 q_2}$ in Fig. 1, are generated by a single parton emission in the last evolution step. (Note that we do *not* account for the non-perturbative “intrinsic k_t ” of the initial partons, represented by a Gaussian distribution with $\langle k_t \rangle < 1$ GeV, for example. In our approach, the transverse momenta of the initial partons is generated entirely perturbatively.)

We use a Sudakov decomposition of the momenta of the two incoming partons:

$$k_i = x_i P_i - \beta_i P_j + k_{i\perp}, \quad (1)$$

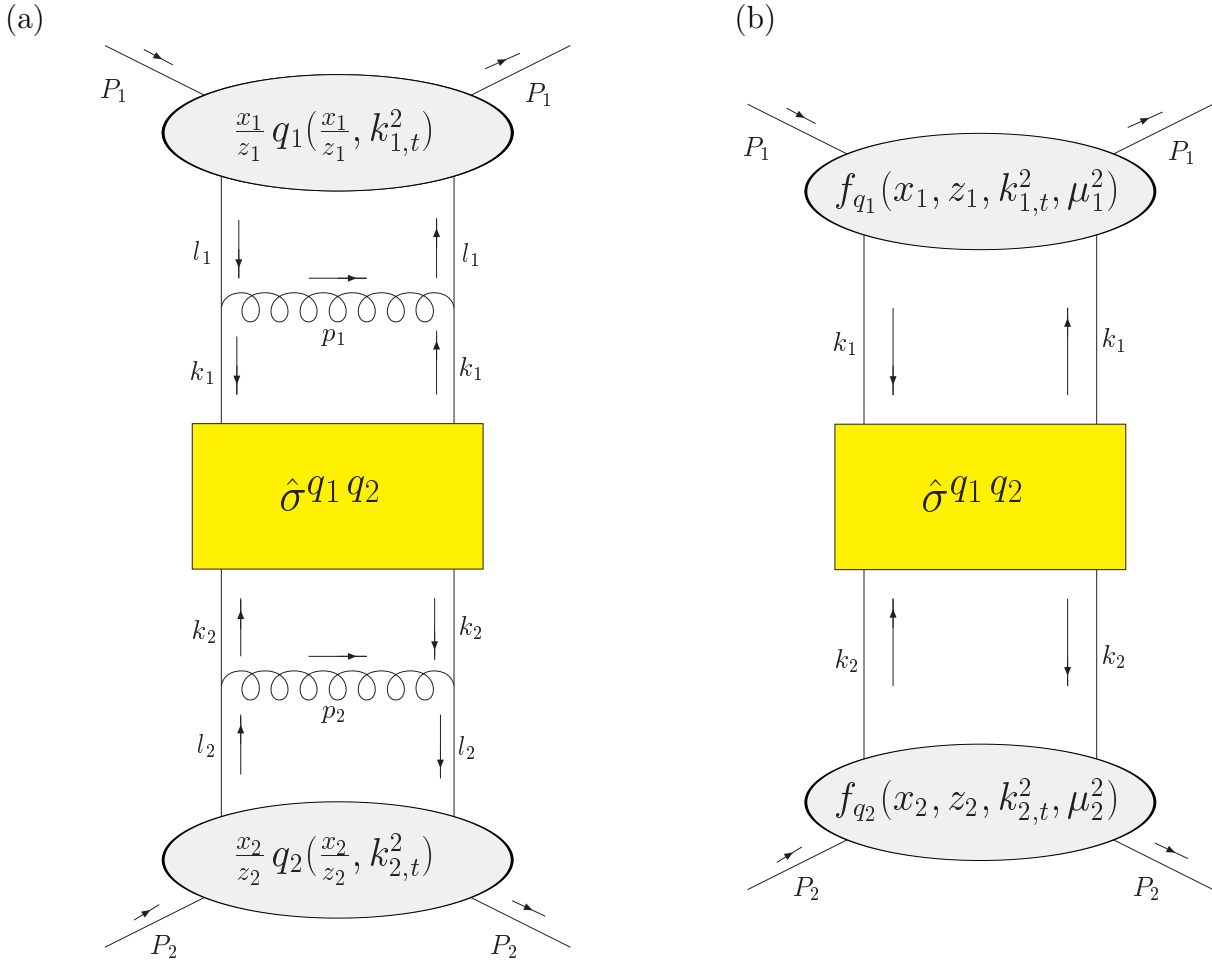


Figure 1: (a) The transverse momentum of each parton entering the subprocess is generated by a single parton emission in the last evolution step. (b) Illustration of (z, k_t) -factorisation: the last evolution step is factorised into $f_{q_i}(x_i, z_i, k_{i,t}^2, \mu_i^2)$, where $i = 1, 2$.

where $(i, j) = (1, 2)$ or $(2, 1)$. We work in the centre-of-mass frame of the colliding hadrons, and neglect the hadron masses so that the squared centre-of-mass energy is $s \equiv (P_1 + P_2)^2 \simeq 2 P_1 \cdot P_2$. Then,¹

$$P_1 = (P_1^+, P_1^-, P_{1\perp}) = \sqrt{s}(1, 0, \mathbf{0}), \quad P_2 = \sqrt{s}(0, 1, \mathbf{0}) \quad \text{and} \quad k_{i\perp} = (0, 0, \mathbf{k}_{i,t}). \quad (2)$$

The penultimate propagators in the evolution ladder have momenta $l_i = x_i P_i / z_i$, so that the partons emitted in the last step have momenta

$$p_i = l_i - k_i = \frac{x_i}{z_i} (1 - z_i) P_i + \beta_i P_j - k_{i\perp}. \quad (3)$$

The on-shell condition for the emitted partons, $p_i^2 = 0$, determines

$$\beta_i = \frac{z_i r_i}{x_i (1 - z_i)}, \quad (4)$$

where $r_i \equiv k_{i,t}^2 / s$, so that the two incoming partons have virtuality $k_i^2 = -k_{i,t}^2 / (1 - z_i)$. The total momentum going into the subprocess labelled $\hat{\sigma}^{q_1 q_2}$ in Fig. 1 is

$$q \equiv k_1 + k_2 = (x_1 - \beta_2) P_1 + (x_2 - \beta_1) P_2 + q_\perp, \quad (5)$$

where $q_\perp = k_{1\perp} + k_{2\perp}$. The kinematic variables obey the ordering:

$$0 < \beta_j < x_i < z_i < 1. \quad (6)$$

If p_i are gluon momenta, then we must impose angular-ordering² constraints due to colour coherence [4]:

$$\xi_1 < \Xi < \xi_2, \quad (7)$$

where $\xi_i \equiv p_i^- / p_i^+$ and $\Xi \equiv q^- / q^+$. That is, the subprocess separates gluons emitted from each of the two hadrons. This condition leads to a suppression of soft gluon emission:

$$z_i < \frac{\mu_i}{\mu_i + k_{i,t}}, \quad (8)$$

with $\mu_1 \equiv x_1 \sqrt{s \Xi}$ and $\mu_2 \equiv x_2 \sqrt{s / \Xi}$.

The partonic cross sections, represented by the rectangles in Fig. 1, depend on x_i , z_i and $k_{i,t}$ through the momentum of the incoming partons k_i (1). Therefore, the partonic cross sections must be convoluted with parton distributions depending on the same variables. We can define DUPDFs $f_a(x, z, k_t^2, \mu^2)$ which satisfy the normalisation condition,

$$\int_x^1 dz \int_0^{\mu^2} \frac{dk_t^2}{k_t^2} f_a(x, z, k_t^2, \mu^2) = a(x, \mu^2), \quad (9)$$

¹The light-cone components of a 4-vector P are $P^\pm \equiv P^0 \pm P^3$.

²“Angular ordering” is in fact a misnomer. It is rapidity ordering which should be applied.

for fixed x and μ , independent of z and k_t . Here, $a(x, \mu^2) = x g(x, \mu^2)$ or $x q(x, \mu^2)$ are the conventional integrated PDFs. Explicit formulae for the DUPDFs were given in [6]. The doubly-unintegrated quark distribution is

$$f_q(x, z, k_t^2, \mu^2) = T_q(k_t^2, \mu^2) \frac{\alpha_S(k_t^2)}{2\pi} \left[P_{qq}(z) \frac{x}{z} q\left(\frac{x}{z}, k_t^2\right) \Theta\left(\frac{\mu}{\mu + k_t} - z\right) + P_{qg}(z) \frac{x}{z} g\left(\frac{x}{z}, k_t^2\right) \right], \quad (10)$$

where $P_{qq}(z)$ and $P_{qg}(z)$ are the unregulated LO DGLAP splitting kernels, and the quark Sudakov form factor is

$$T_q(k_t^2, \mu^2) = \exp\left(-\int_{k_t^2}^{\mu^2} \frac{d\kappa_t^2}{\kappa_t^2} \frac{\alpha_S(\kappa_t^2)}{2\pi} \int_0^{\frac{\mu}{\mu+\kappa_t}} d\zeta P_{qq}(\zeta)\right). \quad (11)$$

The doubly-unintegrated gluon distribution is

$$f_g(x, z, k_t^2, \mu^2) = T_g(k_t^2, \mu^2) \frac{\alpha_S(k_t^2)}{2\pi} \left[\sum_q P_{gq}(z) \frac{x}{z} q\left(\frac{x}{z}, k_t^2\right) + P_{gg}(z) \frac{x}{z} g\left(\frac{x}{z}, k_t^2\right) \Theta\left(\frac{\mu}{\mu + k_t} - z\right) \right], \quad (12)$$

where the gluon Sudakov form factor is

$$T_g(k_t^2, \mu^2) = \exp\left(-\int_{k_t^2}^{\mu^2} \frac{d\kappa_t^2}{\kappa_t^2} \frac{\alpha_S(\kappa_t^2)}{2\pi} \left(\int_{\frac{\kappa_t}{\mu+\kappa_t}}^{\frac{\mu}{\mu+\kappa_t}} d\zeta \zeta P_{gg}(\zeta) + n_F \int_0^1 d\zeta P_{qg}(\zeta)\right)\right), \quad (13)$$

with n_F the number of active flavours.

In terms of the DUPDFs, the hadronic cross section σ is related to the partonic cross sections $\hat{\sigma}^{a_1 a_2}$ by the (z, k_t) -factorisation formula:

$$\sigma = \sum_{a_1, a_2} \int_0^1 \frac{dx_1}{x_1} \int_0^1 \frac{dx_2}{x_2} \int_{x_1}^1 dz_1 \int_{x_2}^1 dz_2 \int_0^\infty \frac{dk_{1,t}^2}{k_{1,t}^2} \int_0^\infty \frac{dk_{2,t}^2}{k_{2,t}^2} f_{a_1}(x_1, z_1, k_{1,t}^2, \mu_1^2) f_{a_2}(x_2, z_2, k_{2,t}^2, \mu_2^2) \hat{\sigma}^{a_1 a_2}. \quad (14)$$

This formula is represented schematically in Fig. 1(b) for the case where the partons a_1 and a_2 are both quarks. The partonic cross sections in (14) are given by

$$d\hat{\sigma}^{a_1 a_2} = d\Phi^{a_1 a_2} |\mathcal{M}^{a_1 a_2}|^2 / F^{a_1 a_2}, \quad (15)$$

where the flux factor $F^{a_1 a_2} = 2 x_1 x_2 s$. The emitted partons with momenta p_i in Fig. 1(a) only factorise from the rest of the diagram, to give the LO DGLAP splitting kernels, in the leading logarithmic approximation (LLA) where only the $dk_{i,t}^2/k_{i,t}^2$ term is kept. Therefore, $|\mathcal{M}^{a_1 a_2}|^2$ must be calculated with the replacement $k_i \rightarrow x_i P_i$ in the numerator in order to keep only this collinear divergent term. However, any propagator virtualities appearing in the denominator of $|\mathcal{M}^{a_1 a_2}|^2$ may be evaluated with the full kinematics, as may the phase space element $d\Phi^{a_1 a_2}$.

For this approach to work, it is vital that the $dk_{i,t}^2/k_{i,t}^2$ term is obtained *only* from ladder-type diagrams like that in Fig. 1(a), and not from interference (non-ladder) diagrams. This

is true if we use a physical gauge for the gluon, where only the two transverse polarisations propagate. For hadron-hadron collisions the natural choice is the planar gauge where the sum over gluon polarisations is performed using

$$d_{\mu\nu}(k) = -g_{\mu\nu} + \frac{k_\mu n_\nu + n_\mu k_\nu}{k \cdot n}, \quad (16)$$

where we take the gauge-fixing vector $n = x_1 P_1 + x_2 P_2$. Such a gauge choice ensures that the $dk_{i,t}^2/k_{i,t}^2$ term is obtained from ladder-type diagrams on *both* sides of the subprocess represented by the rectangle in Fig. 1(a) [7].

A related requirement is that terms beyond the leading $dk_{i,t}^2/k_{i,t}^2$ term, coming from non-ladder diagrams, for example, give a negligible contribution. Such terms are proportional to the Sudakov variable β_i (4) and hence vanish in the limit that $z_i \rightarrow 0$ or $k_{i,t}^2/s \rightarrow 0$ (unless $z_i \rightarrow 1$). Away from these limits it is not obvious that these “beyond LLA” terms will be small, a necessary condition for the factorisation to hold. For the case of inclusive jet production in DIS and working in an axial gluon gauge, it was observed in [6] that the main effect of the extra terms was to suppress soft gluon emission. When the angular-ordering constraint (8) was applied, the extra terms made almost no difference to the cross section. For hadron-hadron collisions, the number of possible non-ladder diagrams is larger, but we see no reason why the same logic cannot be applied. Ultimately, however, we rely on explicit comparison with the data and with more conventional approaches to justify neglecting the non-ladder diagrams.

The DUPDFs in (14) are only defined for $k_{i,t} > \mu_0$, where $\mu_0 \sim 1$ GeV is the minimum scale for which DGLAP evolution of the integrated PDFs is valid. The approximation of the $k_{i,t} < \mu_0$ contribution made in [6] was to take the limit $k_{i,t} \rightarrow 0$ in the kinematic variables (and in $\hat{\sigma}^{a_1 a_2}$), then to make the replacement:

$$\int_{x_i}^1 dz_i \int_0^{\mu_0^2} \frac{dk_{i,t}^2}{k_{i,t}^2} f_{a_i}(x_i, z_i, k_{i,t}^2, \mu_i^2) = a_i(x_i, \mu_0^2) T_{a_i}(\mu_0^2, \mu_i^2), \quad (17)$$

where $T_{a_i}(\mu_0^2, \mu_i^2)$ are the Sudakov form factors (11) and (13). However, a better approximation, which retains the $k_{i,t}$ dependence, is to take the limit $z_i \rightarrow 0$ in the kinematic variables, then to make the replacement

$$\int_{x_i}^1 dz_i f_{a_i}(x_i, z_i, k_{i,t}^2, \mu_i^2) = \frac{k_{i,t}^2}{\mu_0^2} a_i(x_i, \mu_0^2) T_{a_i}(\mu_0^2, \mu_i^2), \quad (18)$$

where we have used (23) of [6].

3 Application to the P_T distribution of electroweak bosons

Perhaps the simplest application of (z, k_t) -factorisation at hadron-hadron colliders is electroweak boson production, where at LO the subprocess is simply $q_1^* q_2^* \rightarrow V$, illustrated in

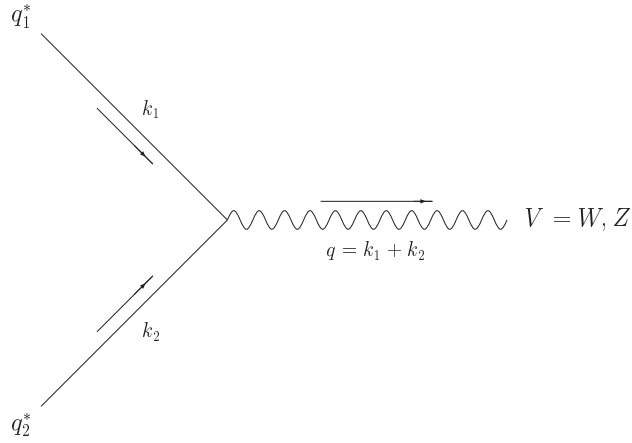


Figure 2: LO Feynman diagram contributing to the P_T distribution of W or Z bosons in the (z, k_t) -factorisation approach.

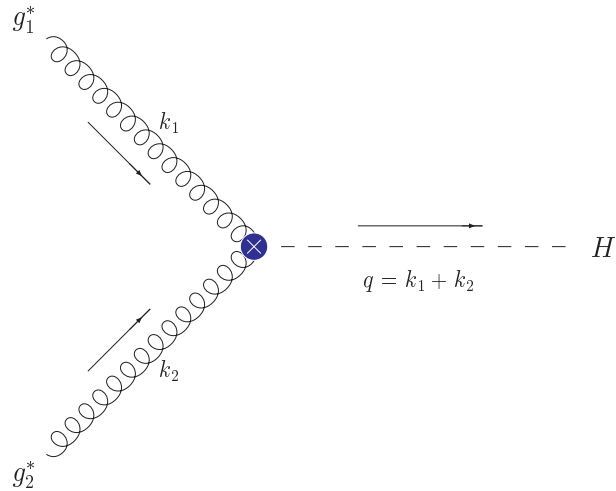


Figure 3: LO Feynman diagram contributing to the P_T distribution of Higgs bosons in the (z, k_t) -factorisation approach. The cross represents the effective vertex in the limit $M_H \ll 2m_t$.

Fig. 2, or $g_1^* g_2^* \rightarrow H$, illustrated in Fig. 3. Here, the ‘*’ indicates that the incoming partons, with momenta k_i given by (1), are off-shell with virtuality $k_i^2 = -k_{i,t}^2/(1 - z_i)$. In the collinear approximation, these diagrams give the Born level estimate of the total cross section σ . When each parton carries finite transverse momentum $\mathbf{k}_{i,t}$, the final electroweak boson has transverse momentum $\mathbf{q}_t = \mathbf{k}_{1,t} + \mathbf{k}_{2,t}$, so we can calculate the P_T distribution

$$\frac{d\sigma}{dP_T} = \sigma \delta(q_t - P_T). \quad (19)$$

The partonic differential cross section for W or Z production is

$$\frac{d\hat{\sigma}}{dP_T}(q_1^* q_2^* \rightarrow V) = \frac{\pi}{N_C} \sqrt{2} G_F M_V^2 V_V^2 \delta(q^2 - M_V^2) \delta(q_t - P_T), \quad (20)$$

where $N_C = 3$ is the number of colours, G_F is the Fermi coupling constant, $V_W^2 \equiv |V_{q_1 q_2}|^2$ is the CKM matrix element squared, and $V_Z^2 \equiv V_q^2 + A_q^2$ is the sum of the vector and axial vector couplings squared.

The dominant production mechanism for SM Higgs production in hadron-hadron collisions is by gluon-gluon fusion via a top quark loop. For the case where $M_H \ll 2m_t$, the well-known effective ggH vertex can be derived from the Lagrangian [8]

$$\mathcal{L}_{\text{eff}} = -\frac{1}{4} \left(1 - \frac{\alpha_S(M_H^2) H}{3\pi v} \right) G_{\mu\nu}^a G^{a\mu\nu}, \quad (21)$$

where $v^2 = (\sqrt{2} G_F)^{-1}$, $G_{\mu\nu}^a$ is the gluon field strength tensor and H is the Higgs field. The partonic differential cross section for SM Higgs production is then

$$\frac{d\hat{\sigma}}{dP_T}(g_1^* g_2^* \rightarrow H) = \frac{\sqrt{2} G_F M_H^2}{576 \pi} \alpha_S^2(M_H^2) \delta(q^2 - M_H^2) \delta(q_t - P_T). \quad (22)$$

For $q_t = 0$, these expressions (20) and (22) are exactly as in the collinear approximation. The difference arises when we consider the precise kinematics:

$$q^2 = s [(x_1 - \beta_2)(x_2 - \beta_1) - R], \quad R \equiv q_t^2/s, \quad (23)$$

$$q_t^2 = |\mathbf{k}_{1,t} + \mathbf{k}_{2,t}|^2 = k_{1,t}^2 + k_{2,t}^2 + 2 k_{1,t} k_{2,t} \cos \phi. \quad (24)$$

Applying the (z, k_t) -factorisation formula (14), the first delta function in (20) and (22) can be used to do the x_2 integration in (14), while the second delta function can be used to do the $k_{2,t}$ integration. In addition, we need to average over the azimuthal angle ϕ between $\mathbf{k}_{1,t}$ and $\mathbf{k}_{2,t}$.

The final hadronic differential cross sections for W or Z production are

$$\begin{aligned} \frac{d\sigma}{dP_T} = & \frac{\pi}{N_C} \sqrt{2} G_F \tau \sum_{x_2=x_2^\pm} \sum_{k_{2,t}=k_{2,t}^\pm} \int_0^1 \frac{dx_1}{x_1} \int_{x_1}^1 dz_1 \int_{x_2}^1 dz_2 \int_0^\infty \frac{dk_{1,t}^2}{k_{1,t}^2} \int_0^{2\pi} \frac{d\phi}{2\pi} \frac{2 P_T \Theta(k_{2,t})}{k_{2,t} |k_{2,t} + k_{1,t} \cos \phi|} \\ & \times \frac{1}{x_1 x_2 - \beta_1 \beta_2} \sum_{q_1, q_2} V_V^2 f_{q_1}(x_1, z_1, k_{1,t}^2, \mu_1^2) f_{q_2}(x_2, z_2, k_{2,t}^2, \mu_2^2), \quad (25) \end{aligned}$$

with $\tau \equiv M_V^2/s$, $k_{2,t}^\pm \equiv -k_{1,t} \cos \phi \pm \sqrt{P_T^2 - k_{1,t}^2 \sin^2 \phi}$, and

$$x_2^\pm \equiv \frac{1}{2x_1} \left\{ \tau + R + x_1 \beta_1 + \frac{z_2 r_2}{1 - z_2} \pm \sqrt{\left(\tau + R + x_1 \beta_1 + \frac{z_2 r_2}{1 - z_2} \right)^2 - 4x_1 \beta_1 \frac{z_2 r_2}{1 - z_2}} \right\}. \quad (26)$$

In practice, the kinematic constraints mean that the $x_2 = x_2^-$ solution does not contribute. The corresponding result for SM Higgs production is

$$\begin{aligned} \frac{d\sigma}{dP_T} = & \frac{\sqrt{2} G_F}{576 \pi} \alpha_S^2(M_H^2) \tau \sum_{x_2=x_2^\pm} \sum_{k_{2,t}=k_{2,t}^\pm} \int_0^1 \frac{dx_1}{x_1} \int_{x_1}^1 dz_1 \int_{x_2}^1 dz_2 \int_0^\infty \frac{dk_{1,t}^2}{k_{1,t}^2} \int_0^{2\pi} \frac{d\phi}{2\pi} \frac{2 P_T \Theta(k_{2,t})}{k_{2,t} |k_{2,t} + k_{1,t} \cos \phi|} \\ & \times \frac{1}{x_1 x_2 - \beta_1 \beta_2} f_g(x_1, z_1, k_{1,t}^2, \mu_1^2) f_g(x_2, z_2, k_{2,t}^2, \mu_2^2), \quad (27) \end{aligned}$$

where $\tau \equiv M_H^2/s$ and $k_{2,t}^\pm$ and x_2^\pm are as above. Note that we have taken the ggH vertex in the $M_H \ll 2m_t$ limit. For $M_H < 2m_t$, the correction to the cross section due to the top quark mass can be approximated [16] by a factor

$$\left[1 + \left(\frac{M_H}{2m_t} \right)^2 \right]^2. \quad (28)$$

The $k_{i,t} < \mu_0$ contribution of (25) and (27) is accounted for using the approximation (18).

4 The K -factor

In the collinear approximation, higher order QCD corrections to the LO diagrams, $q_1 q_2 \rightarrow V$ or $g_1 g_2 \rightarrow H$, are known to be significant when calculating the total cross section. The ratio of the corrected result to the leading order result is the so-called K -factor. A part of these higher order corrections are kinematic in nature, arising from real parton emission, which we have already accounted for at LO in the (z, k_t) -factorisation approach (see Fig. 1). Another part comes from the logarithmic loop corrections which have already been included in the Sudakov form factors (11) and (13). However, we need to include the non-logarithmic loop corrections arising, for example, from the gluon vertex correction to Figs. 2 and 3.

A large part of these non-logarithmic corrections has a semi-classical nature and may be obtained from the analytic continuation of the double logarithm in the Sudakov form factors in going from spacelike (DIS) to timelike (Drell-Yan) electroweak boson momenta [9]. Accounting for the running of the strong coupling α_S , the Sudakov form factors in the DLLA are

$$T_q(k_t^2, \mu^2) = \exp \left(-\frac{C_F}{2\pi b} L \ln L \right) \quad (29)$$

and

$$T_g(k_t^2, \mu^2) = \exp\left(-\frac{C_A}{2\pi b} L \ln L\right), \quad (30)$$

where $L \equiv \ln(\mu^2/\Lambda_{\text{QCD}})$, $b = (33 - 2n_F)/(12\pi)$ and the colour factors are $C_F = 4/3$ and $C_A = 3$.

Replacing μ^2 by $-\mu^2$, we obtain the π^2 -enhanced part of the K -factors:

$$K(q_1^* q_2^* \rightarrow V) \simeq \left| \frac{T_q(k_t^2, -\mu^2)}{T_q(k_t^2, \mu^2)} \right|^2 \simeq \exp\left(C_F \frac{\alpha_S(\mu^2)}{2\pi} \pi^2\right) \quad (31)$$

and

$$K(g_1^* g_2^* \rightarrow H) \simeq \left| \frac{T_g(k_t^2, -\mu^2)}{T_g(k_t^2, \mu^2)} \right|^2 \simeq \exp\left(C_A \frac{\alpha_S(\mu^2)}{2\pi} \pi^2\right). \quad (32)$$

A particular scale choice, $\mu^2 = P_T^{4/3} M_{V,H}^{2/3}$, has been found [10] to eliminate certain sub-leading logarithms in the Sudakov form factors. Therefore, we choose this scale to evaluate $\alpha_S(\mu^2)$ in (31) and (32).

5 Numerical results

The P_T distributions of produced W and Z bosons were measured by the CDF [11] and DØ [12, 13] Collaborations during the Tevatron Run 1, in $p\bar{p}$ collisions at a centre-of-mass energy of $\sqrt{s} = 1.8$ TeV. Measurements were made of $W \rightarrow e\nu$ and $Z \rightarrow ee$ decays, therefore we must multiply the theoretical predictions for W or Z production by the appropriate leptonic branching ratios.³ We use the MRST2001 LO PDFs [15] as input, where $\mu_0^2 = 1.25$ GeV². The final predictions for the P_T distributions (25), integrated over bins of 1 GeV, are shown by the dashed lines in Figs. 4, 5 and 6. The integrated luminosity uncertainty (3.9% for CDF or 4.4% for DØ) is not included in the error bars for the plotted data. The predictions multiplied by the K -factor (31) are shown by the solid lines. Although the K -factor makes up the major part of the discrepancy, we see that the solid lines in Figs. 4, 5 and 6 still underestimate the precise measurements at small P_T to some extent. Normalising to the total measured cross sections by factors 1.26, 1.12 and 1.11, as shown by the dotted lines in Figs. 4, 5 and 6, gives an excellent description of the data over the entire P_T range.

The small discrepancy between the solid lines in Figs. 4, 5 and 6 and the data is easily understood. It was found in [6] that the major higher order corrections to the inclusive jet cross section in DIS could be accounted for by adding extra parton emissions to the LO diagram, $\gamma^* q^* \rightarrow q$. In an axial gluon gauge, ladder-type diagrams gave the dominant contributions. Calculating the $\mathcal{O}(\alpha_S)$ subprocesses $q_1^* q_2^* \rightarrow g V$ and $q_i^* g_j^* \rightarrow q V$ using the (z, k_t) -factorisation prescription would account for the major higher order corrections not already included in the K -factor, and so reduce the observed discrepancy.

³B.R.($W \rightarrow e\nu$) = 0.1072 and B.R.($Z \rightarrow ee$) = 0.03363 [14].

Alternatively, note that the MRST2001 LO PDFs [15] used as input to the last evolution step have been determined by a global fit to data using the conventional collinear approximation. A more precise treatment would fit the integrated PDFs, used as input to the last evolution step, to the proton structure function F_2 , for example, using the (z, k_t) -factorisation formalism at LO. We would expect this treatment to give slightly larger integrated PDFs than the conventional sets by a factor 1.05–1.12, and so eliminate the small discrepancy between the (z, k_t) -factorisation predictions and the data without computing the $\mathcal{O}(\alpha_S)$ subprocesses described above.

The P_T distribution for a SM Higgs boson of mass 125 GeV produced at the LHC ($\sqrt{s} = 14$ TeV) is shown in Fig. 7, where we have multiplied by the factor (28) to approximately account for top quark mass effects. Note that the peak in the Higgs P_T distribution is broader and occurs at a higher P_T than for vector boson production. This is primarily due to the enhanced $g \rightarrow gg$ colour factor ($C_A = 3$) compared to the $q \rightarrow qg$ colour factor ($C_F = 4/3$), resulting in a larger Sudakov suppression at low P_T . By the same reason the K -factor is larger. The P_T distribution is in good agreement with recent, more sophisticated, theory predictions (see, for example, [17]), bearing in mind the spread in the various predictions available due to the different approaches and PDFs used. Evaluating the total cross section by integrating over all P_T gives 39 pb, in exact agreement with a recent soft-gluon resummation calculation at next-to-next-to-leading logarithmic (NNLL) accuracy [18, Fig. 9].

6 Conclusions

We have extended the method of (z, k_t) -factorisation using doubly-unintegrated parton distributions [6] to hadron-hadron collisions. The key idea is that the incoming partons to the subprocess have finite transverse momenta, which can be observed in the particles produced in the final state. This transverse momentum is generated perturbatively in the last evolution step. Virtual terms in the DGLAP equation are resummed into a Sudakov form factor and angular-ordering constraints are applied which regulate soft gluon emission.

We used this framework to calculate the P_T distributions of W and Z bosons produced at the Tevatron Run 1, multiplying by a K -factor to account for the dominant higher order QCD corrections. The predictions gave a very good description of CDF and DØ data over the whole P_T range, after multiplying by an additional overall factor of 1.1–1.3, corresponding to multiplying each DUPDF by ≈ 1.1 . We explained the origin of the need for this extra factor, which should not be regarded as a deficiency of our approach, but rather reflects the fact that the input integrated PDFs should themselves be determined from data using (z, k_t) -factorisation.

We also predicted the P_T distribution for a SM Higgs boson of mass 125 GeV produced at the LHC. Our simple prescription was found to reproduce the predictions of more elaborate theoretical studies [17, 18].

Acknowledgements

I am grateful to Alan Martin and Misha Ryskin for valuable discussions. This work was funded by the UK Particle Physics and Astronomy Research Council.

References

- [1] R. K. Ellis and S. Veseli, Nucl. Phys. B **511** (1998) 649 [arXiv:hep-ph/9706526].
- [2] C. Balazs and C. P. Yuan, Phys. Rev. D **56** (1997) 5558 [arXiv:hep-ph/9704258].
- [3] A. Gawron and J. Kwiecinski, arXiv:hep-ph/0309303.
- [4] M. Ciafaloni, Nucl. Phys. B **296** (1988) 49; S. Catani, F. Fiorani and G. Marchesini, Phys. Lett. B **234** (1990) 339; Nucl. Phys. B **336** (1990) 18; G. Marchesini, Nucl. Phys. B **445** (1995) 49 [arXiv:hep-ph/9412327]; B. Andersson *et al.* [Small x Collaboration], Eur. Phys. J. C **25** (2002) 77 [arXiv:hep-ph/0204115].
- [5] M. A. Kimber, A. D. Martin and M. G. Ryskin, Phys. Rev. D **63** (2001) 114027 [arXiv:hep-ph/0101348]; M. A. Kimber, J. Kwiecinski, A. D. Martin and A. M. Stasto, Phys. Rev. D **62** (2000) 094006 [arXiv:hep-ph/0006184]; M. A. Kimber, A. D. Martin and M. G. Ryskin, Eur. Phys. J. C **12** (2000) 655 [arXiv:hep-ph/9911379].
- [6] G. Watt, A. D. Martin and M. G. Ryskin, Eur. Phys. J. C **31** (2003) 73 [arXiv:hep-ph/0306169].
- [7] Y. L. Dokshitzer, D. Diakonov and S. I. Troian, Phys. Rept. **58** (1980) 269.
- [8] J. R. Ellis, M. K. Gaillard and D. V. Nanopoulos, Nucl. Phys. B **106** (1976) 292; M. A. Shifman, A. I. Vainshtein, M. B. Voloshin and V. I. Zakharov, Sov. J. Nucl. Phys. **30** (1979) 711 [Yad. Fiz. **30** (1979) 1368].
- [9] G. Parisi, Phys. Lett. B **90** (1980) 295; G. Curci and M. Greco, Phys. Lett. B **92** (1980) 175; L. Magnea and G. Sterman, Phys. Rev. D **42** (1990) 4222.
- [10] A. Kulesza and W. J. Stirling, Nucl. Phys. B **555** (1999) 279 [arXiv:hep-ph/9902234].
- [11] T. Affolder *et al.* [CDF Collaboration], Phys. Rev. Lett. **84** (2000) 845 [arXiv:hep-ex/0001021].
- [12] B. Abbott *et al.* [DØ Collaboration], Phys. Rev. D **61** (2000) 032004 [arXiv:hep-ex/9907009].
- [13] B. Abbott *et al.* [DØ Collaboration], Phys. Lett. B **513** (2001) 292 [arXiv:hep-ex/0010026].

- [14] K. Hagiwara *et al.* [Particle Data Group Collaboration], Phys. Rev. D **66** (2002) 010001.
- [15] A. D. Martin, R. G. Roberts, W. J. Stirling and R. S. Thorne, Phys. Lett. B **531** (2002) 216 [arXiv:hep-ph/0201127].
- [16] R. K. Ellis, W. J. Stirling and B. R. Webber, Cambridge Monogr. Part. Phys. Nucl. Phys. Cosmol. **8** (1996) 1.
- [17] W. Giele *et al.*, arXiv:hep-ph/0204316; G. Bozzi, S. Catani, D. de Florian and M. Grazzini, Phys. Lett. B **564** (2003) 65 [arXiv:hep-ph/0302104]; A. Kulesza and W. J. Stirling, arXiv:hep-ph/0307208; A. Kulesza, G. Sterman and W. Vogelsang, arXiv:hep-ph/0309264.
- [18] S. Catani, D. de Florian, M. Grazzini and P. Nason, JHEP **0307** (2003) 028 [arXiv:hep-ph/0306211].

$p\bar{p} \rightarrow Z \rightarrow ee$

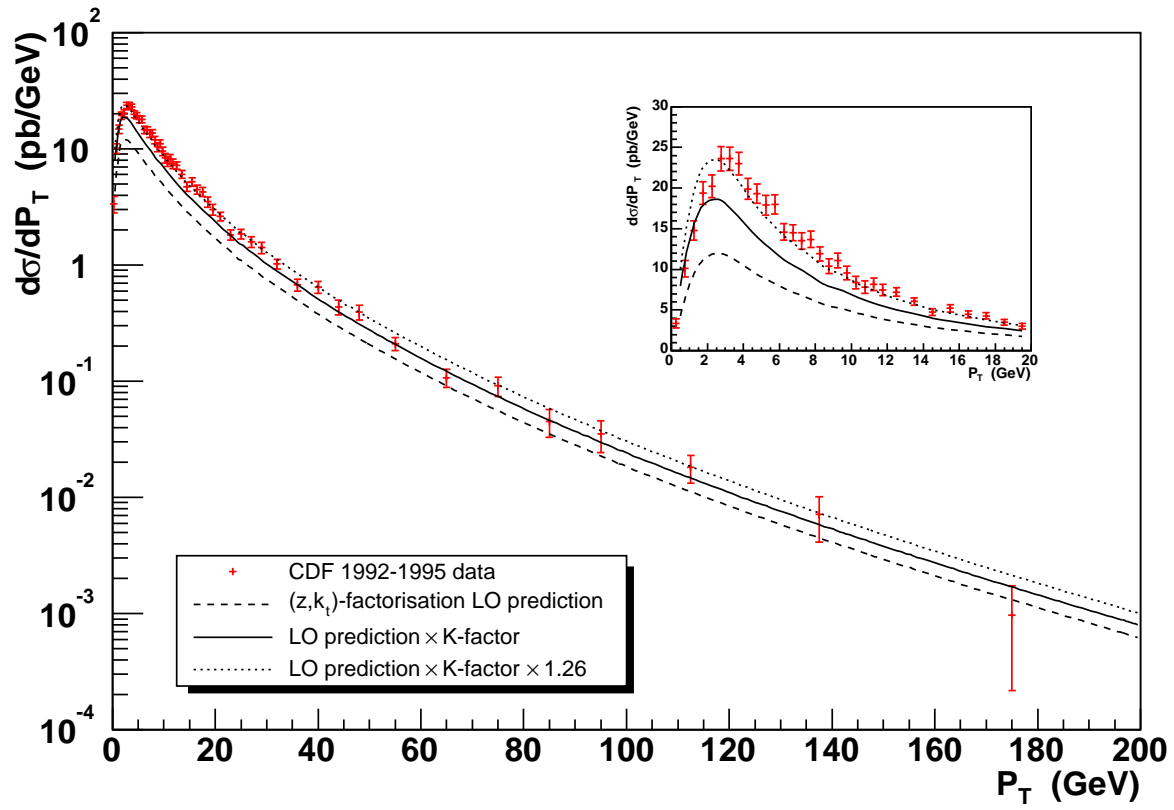


Figure 4: P_T distribution of Z bosons compared to CDF data [11].

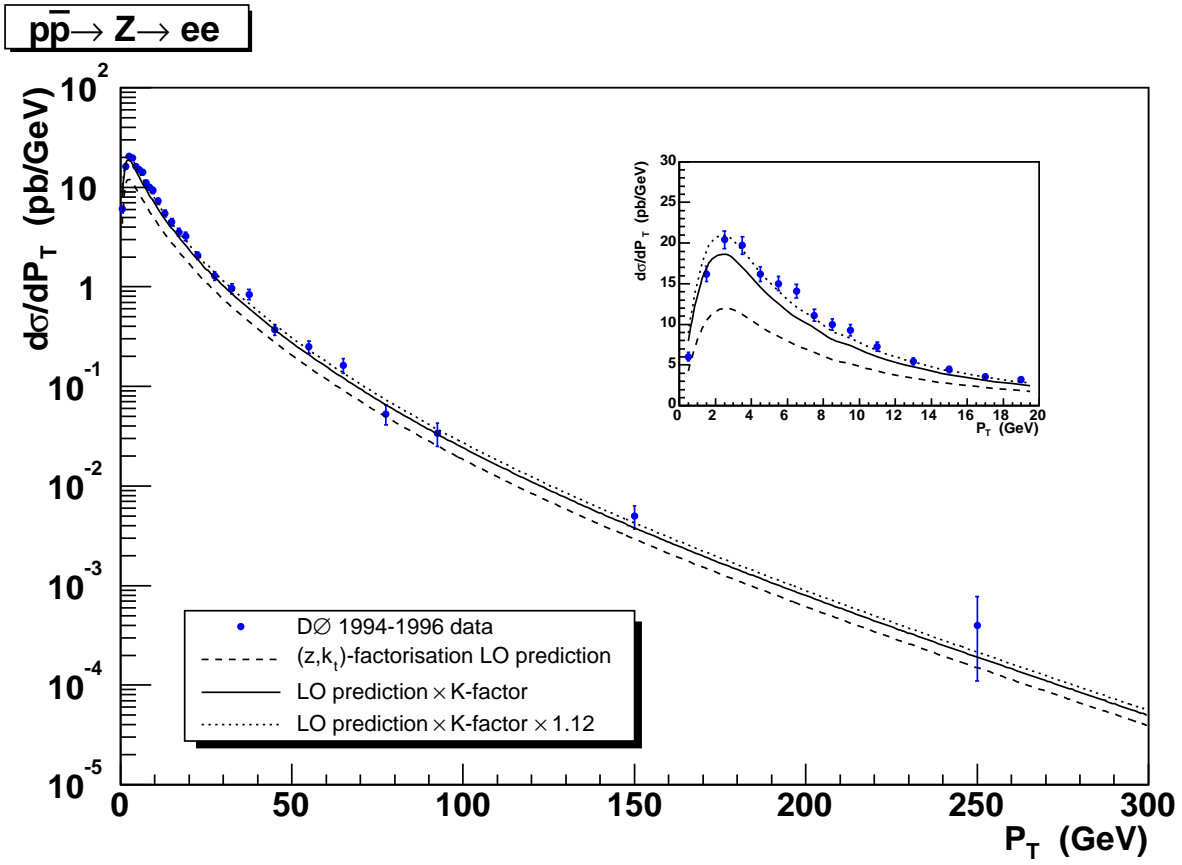


Figure 5: P_T distribution of Z bosons compared to DØ data [12].

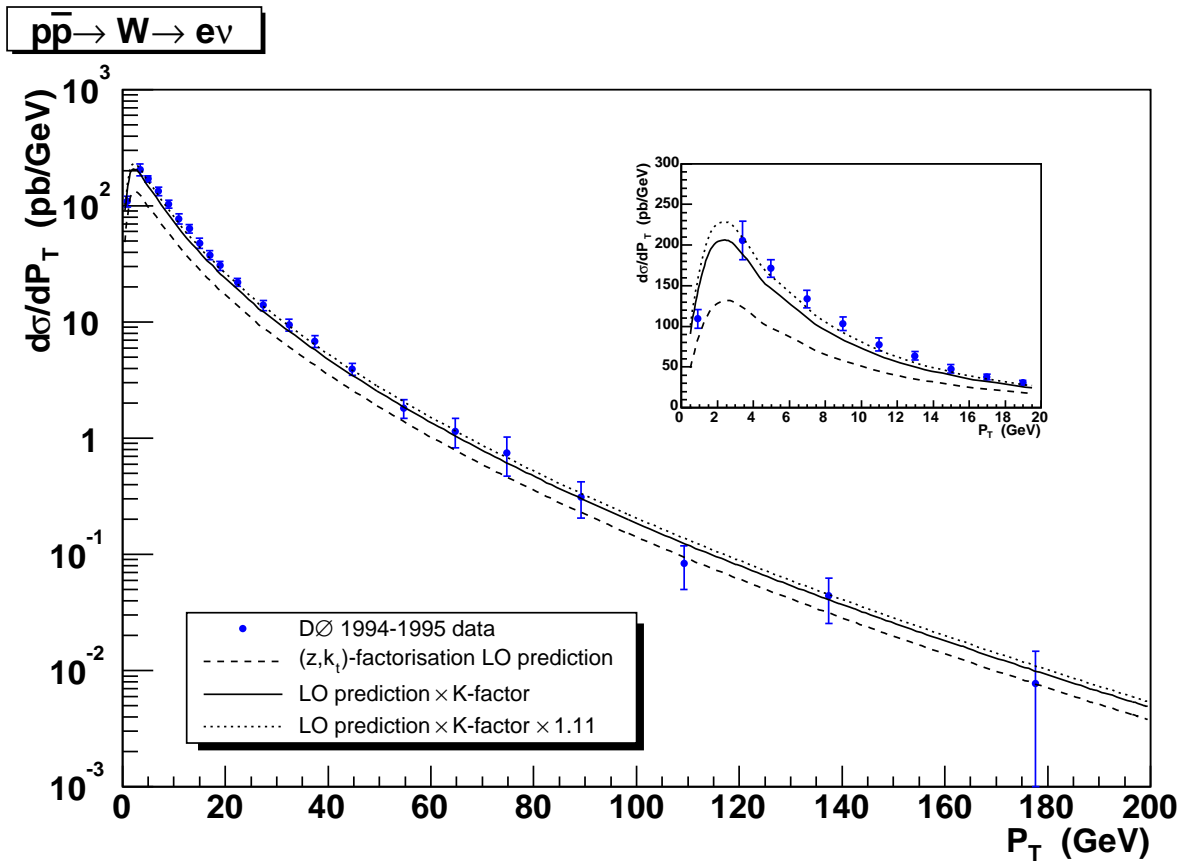


Figure 6: P_T distribution of W bosons compared to DØ data [13].

$pp \rightarrow H$

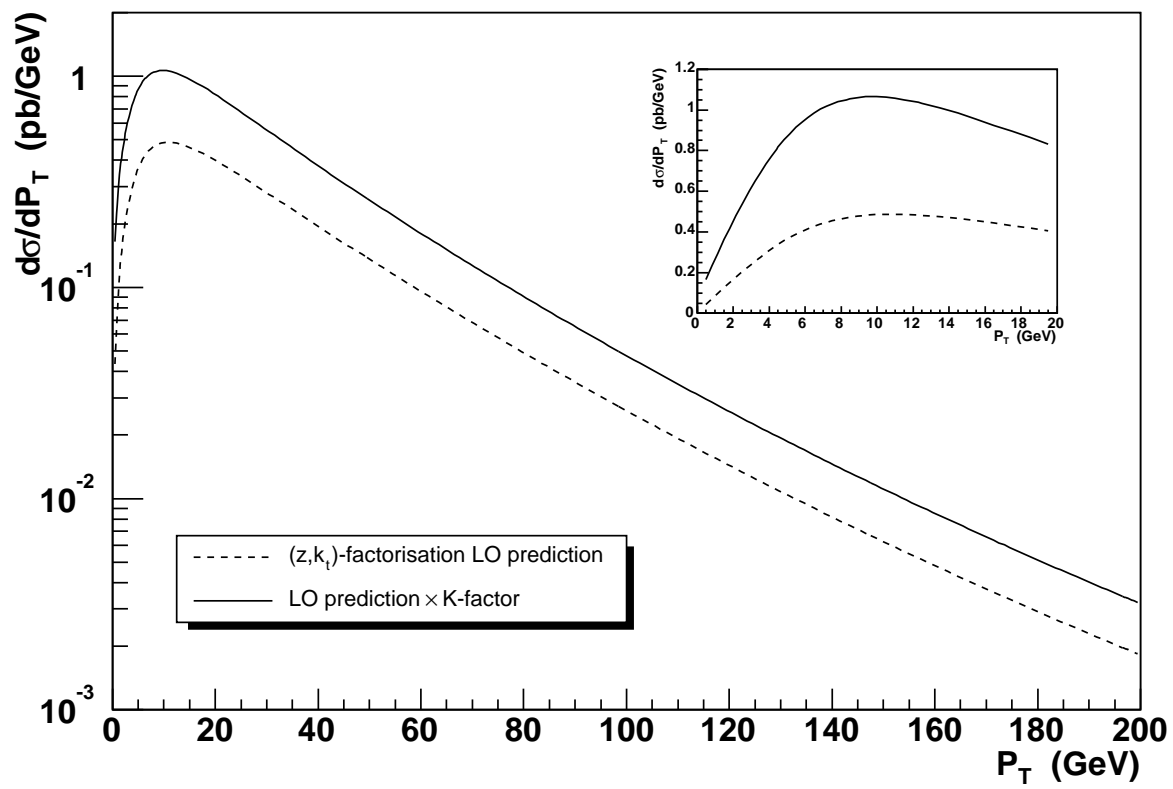


Figure 7: P_T distribution of SM Higgs bosons produced at the LHC with mass 125 GeV.